Spin-orbit splitting and critical point energy at Γ and *L* points of cubic CdTe nanoparticles: Effect of size and nonspherical shape

P. Babu Dayal,[1] B. R. Mehta,[1,*] and P. D. Paulson[2]
[1]*Thin Film Laboratory, Department of Physics, Indian Institute of Technology Delhi, New Delhi 110016, India*
[2]*Institute of Energy Conversion, University of Delaware, Newark, Delaware 19716, USA*
(Received 25 April 2005; revised manuscript received 8 July 2005; published 9 September 2005; publisher error corrected 13 September 2005)

This study reports the observation of changes in critical point energy at Γ and *L* points and an increase in spin-orbit splitting energy of cubic CdTe nanoparticles in comparison to the bulk single-crystal value. ε_1 and ε_2 spectra of CdTe nanoparticles, accurately derived from spectroscopic ellipsometry measurements on CdTe nanoparticles dispersed in SiO_2 films, show E_0, $E_0+\Delta_0$, E_1, and $E_1+\Delta_1$ critical points at 1.75, 2.74, 3.29, and 3.83 eV, respectively. Glancing-angle x-ray diffraction and high-resolution transmission electron microscopy investigations confirm cubic CdTe nanoparticles with good crystallinity and a nonspherical shape. Variable magnitudes of size-induced stress along the minor and major axes cause dissimilar shifts of heavy-hole and split-off bands resulting in a positive contribution to spin-orbit splitting energy, in addition to the small size.

DOI: 10.1103/PhysRevB.72.115413 PACS number(s): 78.67.Bf

INTRODUCTION

Spin-orbit (SO) splitting is an essential characteristic of the electronic band structure of semiconductor materials.[1] It arises due to the interaction of the intrinsic magnetic moment of the electron spin with the magnetic field generated by electron motion. The magnitude of the SO splitting is known to affect the location of the lowest hole levels in the valence band of microcrystals and thus any change in SO splitting is bound to affect the luminescent properties of semiconductors.[2] In cubic and hexagonal crystals, the three valence bands $(j,m_j)=(3/2,\pm 3/2)$, $(3/2,\pm 1/2)$, and $(1/2,\pm 1/2)$ are called the heavy-hole (*A*), light-hole (*B*), and split-off hole (*C*) subbands, respectively.[3] The crystal-field splitting between *A* and *B* subbands arises due to the anisotropy of the hexagonal structure. In cubic crystal structures, the doubly degenerate *A* and *B* bands (the crystal-field splitting is zero) and a lower nondegenerate *C* band are separated by the SO splitting. In bulk and thin-film semiconductors, modifications in crystal structure due to stress or lattice distortion influence the magnitude of the SO splitting.[4,5] Some theoretical work has been carried out to study the effect of nanoparticle size and shape on *A*, *B*, and *C* subbands in Cd*X* (*X*=S, Se, and Te) nanoparticles.[1,3,6,7] Using the multiband effective-mass approximation, Efros *et al.* theoretically showed a possible increase (or decrease) of crystal-field splitting in oblate- (or prolate-) shaped CdSe nanoparticles and also predicted a mixing of *A*, *B*, and *C* bands due to shape anisotropy.[1] Empirical pseudopotential calculations carried out by Tomasulo *et al.* on Cd*X* nanoparticles clearly show increase in the energy of *A*, *B*, and *C* subbands at reduced dimensions.[3] Although the optical properties of II-VI semiconductors are probably the most widely investigated nanoparticle characteristic, these experimental studies are limited to the size-induced shift in the fundamental absorption edge.[6–12] The present study reports on the experimental investigation of the effect of nanoparticle size and shape on the critical point transitions at the Γ and *L* points and SO splitting energy in any nanoparticle system. The spectroscopic ellipsometry (SE) technique has been used to obtain the ε_1 and ε_2 spectra of CdTe nanoparticles from the measurements carried out on CdTe nanoparticles dispersed in SiO_2 films.

It may be mentioned here that nanoparticles dispersed in a SiO_2 matrix represent an ideal configuration for studying the optical properties of nanoparticles, as the SiO_2 matrix provides a protective environment to the nanoparticle surface right from its early stages of growth and its transparent nature makes optical characterization easy. In various reports on the optical properties of nanoparticles dispersed in the SiO_2 matrix, the size-dependent shift of the fundamental absorption edge has been determined directly from the absorbance spectra or from the Tauc plots drawn from transmission and reflectance data or their derivatives.[8–12] Factors like surface roughness, interference, and thickness nonuniformity and the presence of the matrix have been completely ignored.

EXPERIMENT

CdTe nanoparticles dispersed in SiO_2 films (CdTe:SiO_2 samples) have been grown by the magnetron sputtering technique. High-quality elemental Cd and Te targets have been fixed onto a 2-in. diameter SiO_2 slab for depositing CdTe:SiO_2 films. Argon partial pressure of 3.75×10^{-2} Torr at a flow rate of 10 SCCM (SCCM denotes cm^3/min at STP) is maintained during sputtering. A power of 120 W from a 13.56 MHz rf generator has been used for sputtering. Substrate rotation at 8 rpm has been employed to achieve deposition uniformity. Samples A2, A4, and A6 have been formed by postdeposition heat treatment of as-deposited CdTe:SiO_2 samples (sample A0) in vacuum at 5×10^{-6} Torr at temperatures 200, 400, and 600 °C, respectively. A conventional transmission electron microscope (TEM) JEOL JEM 200 CX and a high-resolution field-emission transmission electron microscope 2010 UHR-

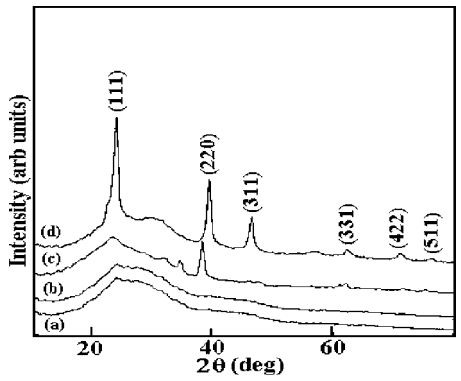

FIG. 1. GAXRD spectra of (curve *a*) as-deposited (A0) and vacuum annealed samples (curve *b*) A2, (curve *c*) A4, and (curve *d*) A6.

JEOL (resolution=0.14 nm) at 200 keV have been used to study the crystal structure, size, and shape of the CdTe nanoparticles. A variable-angle spectroscopic ellipsometer VASE® (J. A. Woollam Co., Inc.) at 57.5°, 62.5°, and 67.5° incident angles in the 0.725–4.6 eV photon energy range has been used for carrying out SE measurements. VASE is a rotating-analyzer ellipsometer equipped with an autoretarder, which is useful for measuring the depolarization caused by surface roughness, thickness nonuniformity, and backside reflection from the glass substrate.

RESULTS AND DISCUSSIONS

Figure 1 shows the glancing-angle x-ray diffraction (GAXRD) spectra of $CdTe:SiO_2$ samples A0, A2, A4, and A6. Curves *a* and *b* in Fig. 1 indicates that samples A0 and A2 are amorphous in nature. In the GAXRD spectrum of sample A4 (curve *c*), peaks corresponding to the cubic CdTe start appearing. The spectrum of the A6 sample (curve *d*) shows predominantly peaks corresponding to the cubic (fcc) phase of CdTe. The (*hkl*) values assigned to peaks corresponding to the cubic CdTe are in agreement with standard JCPDS values.[13] The above results and TEM analysis of these samples show that well-defined CdTe nanoparticles are formed at annealing temperature of 600 °C.[14] It may also be mentioned that the crystallization temperature for CdTe is around 565 °C.[15]

Using SE, the analysis was carried out in two steps. In the first step, the effective optical functions of the $CdTe:SiO_2$ matrix were determined by a three-layer optical model (glass substrate+$CdTe:SiO_2$ layer+surface roughness) separating the absorption due to the glass substrate. The three-layer optical model used for this analysis is shown in Fig. 2. Since the extinction coefficient of the samples is negligibly small in the wavelength region $\lambda < 1.5$ eV, the refractive index and thickness of the $CdTe:SiO_2$ matrix were the only two unknown parameters that needed to be determined. At the same time we are measuring two unknowns (δ and ψ) over a large energy range at multiple incident angles. Hence a regression analysis that satisfies multiple data sets would provide a very accurate thickness value. After obtaining the thickness of the $CdTe:SiO_2$ layer, the optical constants for

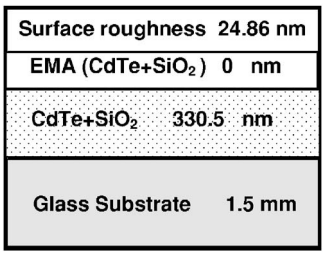

FIG. 2. Four-layer optical model used to simulate the optical constants. EMA ($CdTe+SiO_2$) layer is a dummy layer with a zero thickness, which provides variable optical functions to the EMA layer. The maximum thickness variation will be ±0.5 nm. In the absence of the dummy layer, the model serves as three-layer model.

the spectral regions are obtained using a point-by-point fit starting from the transparent region. By using the obtained thickness and refractive index values in the transparent region, a wavelength-by-wavelength fit was performed over the entire spectral region and the values of optical functions were determined in the whole energy range. The optical function spectrum was further refined by regression analysis using a general oscillator layer created from the starting spectra. A general oscillator layer consisting of a Gaussian-broadened polynomial superposition semiconductor oscillator and several harmonic oscillators was used to simulate different electronic transitions in the optical spectra.[16] The optical constants of the $CdTe:SiO_2$/glass structure were generated using this general oscillator layer incorporated in the above mentioned three-layer optical model. Software employing the Levenberg-Marquardt algorithm was used to minimize error between the fitted and the measured data.[16] By using the experimental standard deviation as the weighting parameter in the fit, the contributions due to noise in the mean square error are reduced significantly. A detailed description of this can be found elsewhere.[17,18] The ε_2 spectrum thus obtained is due to CdTe nanoparticles and is shown as a simulated curve in Fig. 3. Our earlier studies have shown the presence of a 1–2 nm thick amorphous $CdTeO_3$ layer around CdTe nanoparticles.[19] Due to the large band gap of $CdTeO_3$ (3.98 eV) and small shell thickness, the contribution of $CdTeO_3$ to the dielectric structure of CdTe nanoparticles is expected to be insignificant. It will also be too complicated to take it into account in the optical model.

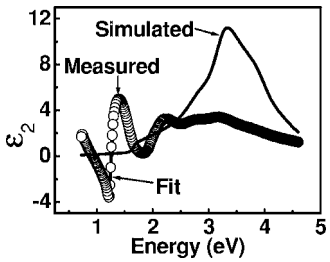

FIG. 3. Curve with open squares (□) represents the simulated values of ε_2 corresponding to CdTe nanoparticles. These simulated values provide a match between the measured (○) and fitted (line) values of ε_2 spectra corresponding to CdTe nanoparticles dispersed in SiO_2 samples.

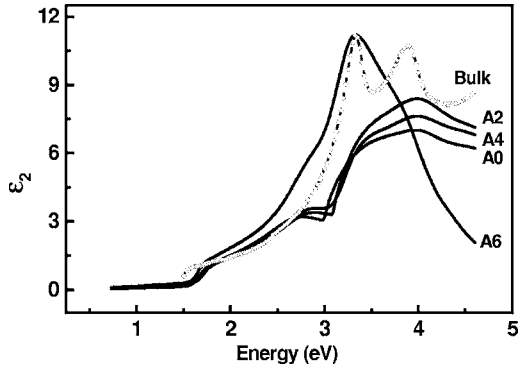

FIG. 4. ε_2 spectra of samples A0, A2, A4, A6, and bulk CdTe.

In the second step the optical constants of the CdTe nanoparticles are determined using the effective-medium (EMA) approximation. In this step, the optical functions of CdTe nanoparticles are determined again using a three-layer optical model. This is similar to the three-layer model for the optical constants of $CdTe+SiO_2$ described in the first step except the EMA layer using Maxwell-Garnett approximations. In this model the $CdTe+SiO_2$ becomes a dummy layer with zero thickness, which provides variable optical functions (oscillator model) to EMA layer. This model takes into account the optical constants of $CdTe+SiO_2$ matrix and the optical properties of bulk SiO_2.[20] Here the volume fraction of the SiO_2 matrix obtained from x-ray photoelectron spectroscopy measurement (e.g., the value for $CdTe:SiO_2$ is 12:88 in sample A6, i.e., the cubic nanoparticle sample A6) is used as an input parameter.[19] The oscillator strength along with broadening are taken as fit parameters. Again the data fit is carried out simultaneously on three incident angles to improve the confidence limit in the data fit.

In Fig. 4, the fitted ε_2 spectra of samples A0, A2, A4, and A6 have been compared with the ε_2 spectrum of bulk CdTe. A comparison of the fitted ε_1 and ε_2 spectra of CdTe nanoparticles with that of bulk CdTe shows that the dielectric function spectra of A0, A2, and A4 are quite different from the bulk spectra. These observations are also consistent with the GAXRD and TEM results discussed earlier, which show that CdTe nanoparticles in these samples are not well formed. The ε_1 and ε_2 spectra sensitively depend on the crystallinity, stoichiometry, and particle size. Therefore, the spectra for sample A6, which comprises well-crystallized cubic CdTe nanoparticles, have been discussed in detail. In the dielectric function spectra of nanoparticles shown in Fig. 5,

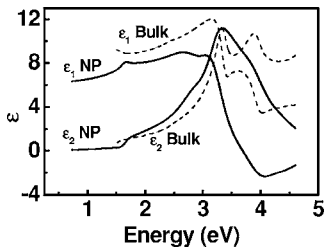

FIG. 5. Fitted ε_1 and ε_2 spectra of CdTe nanoparticles (NP) (solid lines) and bulk (dashed lines).

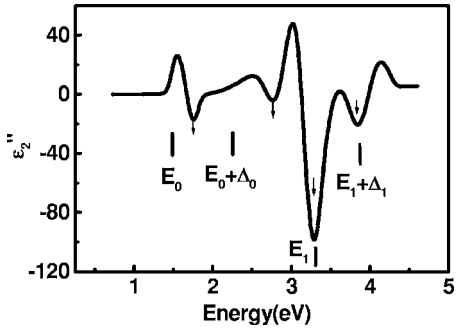

FIG. 6. Simulated ε_2'' spectra of CdTe nanoparticles showing the position of critical point transitions. Vertical bars denote critical point transitions in bulk CdTe (Ref. 13). Arrows indicate the values corresponding to CdTe nanoparticles.

the ε_1 value is lower than the corresponding bulk value in the complete energy range. The ε_2 values of CdTe nanoparticles in the energy range 1–3 eV are similar to bulk values, whereas at energy higher than 3 eV, the ε_2 values are significantly lower than the bulk values. It is well known that the complex dielectric response is the manifestation of different interband transitions through Kramer-Kronig relations. The optical transitions depend on the energy band structure through the imaginary part of the dielectric constant (ε_2). Hence the dielectric constant is directly proportional to the optical joint density of states between valence and conduction band states.[21] Since the joint density of states in the case of nanoparticles is lower than for the corresponding bulk materials due to the lesser number of electronic states available due to small size, it is expected that the ε_2 values in case of nanoparticles will be lower in comparison to single-crystal bulk values.[22] In addition, the surface polarization effects due to induced charges at the nanoparticle-matrix interface can also reduce these values.[23] The modified Penn model also predicts a decrease in the dielectric constant with size.[24] Critical points in the second derivative of the ε_2 spectrum correspond to the energy at which the joint density of states shows a strong variation as a function of energy. These critical point energies were identified by the minimum negative value of the second derivative of ε_2 (ε_2'') as shown in Fig. 6.[17,18,25] The ε_2'' spectra of the CdTe nanoparticles show four critical points E_0, $E_0+\Delta_0$, E_1, and $E_1+\Delta_1$ at 1.75, 2.74, 3.29, and 3.83 eV, respectively. These critical points correspond to the allowed transitions Γ_8^v-Γ_6^c, Γ_7^v-Γ_6^c, $L_{4,5}^v$-L_6^c, and L_6^v-L_6^c levels in the electronic band structure of CdTe. E_0 is the optical absorption gap of CdTe at the Γ point and E_1 is the absorption edge at the L point corresponding to the center and edge of the first Brillouin zone, respectively. Figure 7 shows the nonlinear curve fits of the second derivatives of the real and imaginary parts of the dielectric function in the energy range corresponding to the critical points E_0, $E_0+\Delta_0$, E_1, and $E_1+\Delta_1$ using the procedure adopted by Lautenschlager *et al.*[26] It may be mentioned here that the degree of divergence (χ^2) between experimental and fitted data points is less than 3 and the accuracy of the energy positions of the critical points obtained from the fitted curve is less than ±3.0 meV. The critical point energy positions and corresponding shift with respect to bulk values are summarized in Table I. The E_0 and

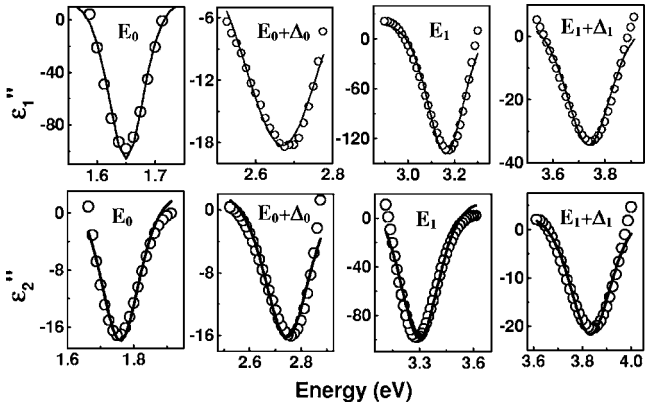

FIG. 7. Nonlinear best-fit curves for second derivatives of ε_1 and ε_2 spectra. E_0 and $E_0+\Delta_0$ are the critical point transitions at the Γ point and E_1 and $E_1+\Delta_1$ are the critical point transitions at the L point.

$E_0+\Delta_0$ energies are blue-shifted with respect to the corresponding bulk values of 1.5 and 2.3 eV, respectively. It is important to mention here that there is a scatter in the energy positions of the critical points reported in the literature, which may be due to differences in the measurement method, measurement temperature, or sample conditions. Values obtained from reflectance measurements at 293 K on single-crystal CdTe have been taken as the standard bulk values.[27] The observed shift in E_0 of about 250 meV is similar to the values (300 meV for 10 nm size) calculated for CdTe nanoparticles using the tight-binding approximation in accordance with a $1/D^{1.42}$ dependence with D as the nanoparticle diameter.[28] The shift in $E_0+\Delta_0$ is about 440 meV in comparison to the bulk value. In contrast to E_0 and $E_0+\Delta_0$, the energy values of the E_1 and $E_1+\Delta_1$ transitions show negligible shifts of about 30 and 60 meV, respectively, with respect to the bulk values. This may be due to weak confinement at the L point. At nanoparticle dimensions smaller than or comparable to the Bohr excitonic radius, a size-dependent change in energy level takes place due to strong-confinement effects. In this strong-confinement regime, the positions of quantum levels are described by motions of the electron and hole, separately.[1] At dimensions larger than the Bohr excitonic radius, the confinement of the electron-hole pair is very weak and size-dependent changes in energy levels are relatively smaller.[1] In the case of CdTe, the Bohr exciton radii for A and B subbands of CdTe at the L point are 0.60 and 0.65 nm, respectively. In comparison to this, the value of the Bohr radius at the Γ point is 6.50 nm.[29] At CdTe nanoparticle diameter of 8.5 nm that is significantly higher than the Bohr exciton radius at the L point, so the effect of confinement is expected to be very weak. This explains the small shifts observed in the E_1 and $E_1+\Delta_1$ transition energy levels.

As already mentioned, there are not many experimental or theoretical works on the effect of nanoparticle character on SO splitting and critical point transitions at the L point. There is only one theoretical study on this subject in which the effect of size on individual A, B, and C subbands in CdX nanoparticles has been investigated using empirical pseudopotential calculations.[3] According to these calculations, in hexagonal CdS and CdSe nanoparticles, the size-induced

TABLE I. The values of the critical point energy of CdTe bulk (Ref. 4) and curve fits of the second derivative of the ε_2 spectrum of nanoparticle sample A6.

Sample[a]	E_0	$E_0+\Delta_0$	Δ_0	E_1	$E_1+\Delta_1$	Δ_1
Bulk (eV)	1.50	2.30	0.80	3.32	3.89	0.57
NP (eV)	1.75	2.74	0.99	3.29	3.83	0.55
Shift (meV)	250	440	190	−30.0	−60.0	−30.0

[a]Energies of critical point transitions are experimentally measured values at 293 K (Ref. 13).

shifts in the positions of A and C subbands are similar and hence the net change in SO splitting due to size is quite small. However, in the case of cubic CdTe nanoparticles, the size-dependent change of individual A, B, and C subbands increases by different magnitudes and hence the SO splitting increases in comparison to the single-crystal bulk value. For a diameter of 4 nm, the increase in SO splitting is predicted to be about 300 meV. The change in SO splitting decreases with increase in size and becomes negligible at nanoparticle diameter larger than 10 nm. In the case of CdSe having the hexagonal structure, the multiband effective-mass approximation predicts an additional contribution to the crystal-field splitting in nonspherical nanoparticles due to anisotropy in the hole effective-mass values.[1] In the case of CdTe nanoparticles having the highly symmetric cubic structure, the electron and hole effective masses are identical along different crystallographic directions.[23] However, the electron and hole effective-mass values can change due to the presence of stress or lattice distortions. It is well known that enhanced surface-to-volume ratio at reduced dimensions results in size-induced stress or lattice distortion. A gradual decrease in lattice constant with decreasing nanoparticle size has been shown in the case of CdSe nanoparticles, which is related to the surface energy through the Laplace law.[30,31] With reduction in size, the percentage of surface atoms increases and thus the average surface pressure per atom increases. This can be understood in terms of the liquid drop model[32] and bond-length, order, and strength correlations.[33] In nonspherical nanoparticles, the magnitude of size-induced stress will be different along the minor and major axes. Thus, it is important to consider the effect of stress on the positions of A, B, and C bands for describing the effect of shape on the SO splitting. The effect of stress along the [100] and [111] directions on the splitting between A and B subbands has been studied in the case of single-crystal CdTe.[34] According to this study, two deformation potentials are required to describe the splitting between A and B bands in the case of strained cubic CdTe crystals having an elastic anisotropy factor of 2.39. This can result in a crystal-field splitting of the order of 15–20 meV. It has also been shown that a small amount of tensile stress (about 2.3×10^9 N/m^2) due to the presence of oxygen atoms can break the degeneracy of A and B bands in cubic CdTe nanoparticles.[35] As already mentioned, the magnitude of the size-induced stress in nonspherical nanoparticles will be relatively larger along the smaller dimension. A quasicubic model has been used to calculate the effect of stress along different directions on the band structure of

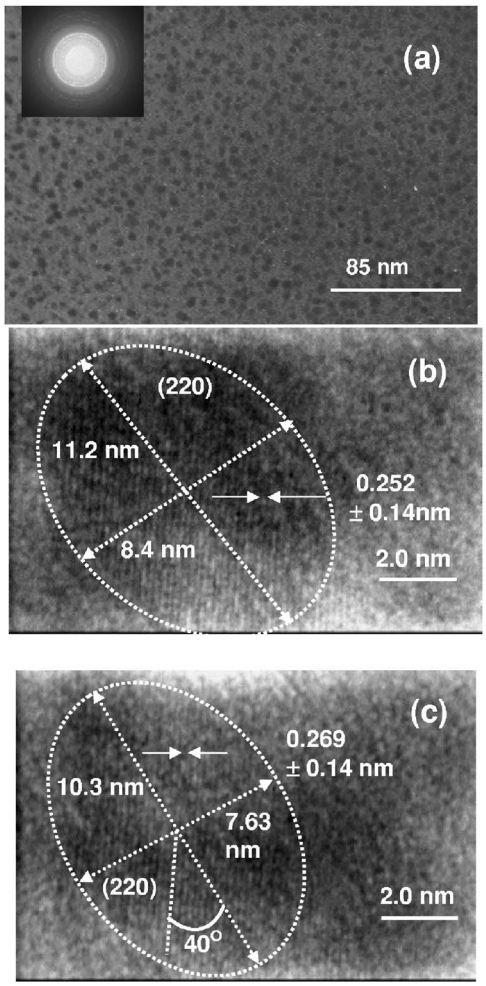

FIG. 8. (a) TEM image showing CdTe nanoparticles dispersed in SiO_2 sample. (b), (c) Typical HRTEM images showing the nonspherical shape of CdTe nanoparticles. Nanoparticle dimensions along major and minor axes are also shown. Plane (220) is oriented at ~40° with respect to major axis. Major (x) and minor (y) axes have dimensions of 10–11 and 7–9 nm and the average diameter $(y^2x)^{1/3}$ of the nonspherical nanoparticles is ~8.5 nm.

nearly cubic crystals.[36] These calculations show that the relative strength of transitions involving A and C bands is modified differently on application of stress along different directions but having the same magnitude. If the magnitude of stress applied along different directions is different, the above effect will be enhanced further. This explains the large contribution to the SO splitting due to the nonspherical shape of the CdTe nanoparticles.

A TEM micrograph of the $CdTe:SiO_2$ sample given in Fig. 8(a) shows CdTe nanoparticles dispersed in SiO_2 matrix. Typical high-resolution TEM (HRTEM) lattice images of CdTe nanoparticles in the above sample are also shown in Figs. 8(b) and 8(c). The HRTEM lattice images of nanocrystals have been analyzed using image processing and analysis (IMAGEJ 1.32) software. The HRTEM images clearly demonstrate that CdTe nanoparticles are well crystallized without any crystallographic defects and are nonspherical in shape. The shape of the nanoparticles can be approximately described as an ellipsoid with major and minor axes having

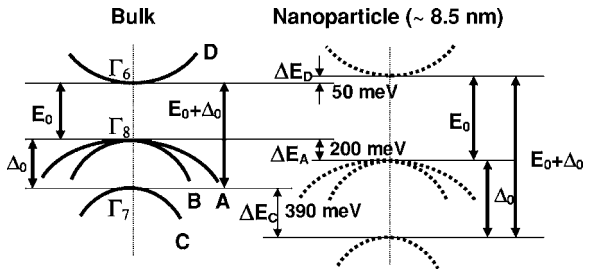

FIG. 9. Schematic diagram showing the comparison of the band structure of bulk CdTe (solid curves) and CdTe nanoparticles (dotted curves). Heavy-hole, light-hole, and split-off hole subbands are denoted as A, B, and C bands, respectively. For clarity, the conduction band is denoted as the D band. Based on the result of the present study, the critical point transitions E_0 and $E_0+\Delta_0$, SO splitting Δ_0, shifts in conduction band (ΔE_D), heavy hole (ΔE_A), and split-off subbands (ΔE_C) are also shown.

dimensions 10–11 nm and 7–9 nm, respectively. As shown in Figs. 8(b) and 8(c), the (220) planes are oriented at about a 40° angle with the major axis. It is quite probable that the (111) plane, which makes an angle of 35.11° with the (220) plane, forms the major axis. In bulk CdTe single crystals, it has been shown that the growth rate is higher along ⟨111⟩ directions.[37] The HRTEM studies carried out on CdS and CdSe nanoparticles dispersed in a glass matrix have shown that the difference in growth rate along different crystallographic directions results in the evolution of nonspherical crystals in nanoparticles having size below 10 nm and annealing temperature lower than 700 °C.[38] X-ray diffraction studies carried out on Si nanoparticles have also shown that different growth rates of Si nanoparticles along the [001] and [100] directions result in nonspherical shapes.[31]

The effect of nanoparticle character on the band structure of CdTe is schematically described in Fig. 9. The shift in the conduction band (D band) and valence band (A subband) has been obtained from the experimentally determined value of ΔE_0 and the theoretically calculated ratio of the shift in the conduction and valence bands ($\Delta E_D/\Delta E_A$). Tight-binding calculations carried out on Si nanoparticles having 4 nm size show the $\Delta E_D/\Delta E_A$ ratio to be about 2, which increases with increase in size.[39] We have used a value 4 (for 8.5 nm nanoparticles) for estimating ΔE_D and ΔE_A.[40] The shift in the position of the C subband (ΔE_C) can also be estimated from the shift in the position of the $E_0+\Delta_0$ transition (440 meV) and ΔE_D. Here the $\Delta E_C/\Delta E_A$ ratio is found to be of the order of 2. It is interesting to note that the effect of the nanoparticle nature on the position of the C subband is greater in comparison to the A subband, probably due to the higher overlap of the electron and split-off hole wave functions (in accordance with pseudopotential calculations[3]) and the smaller effective-mass value of the split-off hole (in accordance with the effective-mass approximation[1]). Thus, the increase in SO splitting energy observed in CdTe nanoparticles is due to the size of the CdTe nanoparticles being of the order of the Bohr exciton radius at the Γ point and the nonspherical shape resulting in different magnitudes of stress along the minor and major axes.

In conclusion, the ε_1 and ε_2 spectra of CdTe nanoparticles derived from SE measurements on $CdTe:SiO_2$/glass

samples show lower dielectric function values, especially at energy greater than 3 eV. The ε_2'' spectrum for CdTe nanoparticles shows the position of four critical points E_0, $E_0+\Delta_0$, E_1, and $E_1+\Delta_1$ at 1.75, 2.74, 3.29, and 3.83 eV, respectively. The effect of confinement has been observed to be stronger at the Γ point than at the L point. The observed increase of SO splitting in CdTe nanoparticles with respect to the bulk value has been explained due to the combined effect of size and nonspherical shape. HRTEM investigations show that CdTe nanoparticles have dimensions of 10–11 and 7–9 nm along the major and minor axes, respectively. Variable magnitudes of size-induced stress along the major and minor axes cause dissimilar shifts of heavy and split-off hole bands with $\Delta E_C/\Delta E_A$ of the order of 2.

ACKNOWLEDGMENTS

We acknowledge financial support from the Board of Research in Nuclear Sciences, Mumbai, India to carry out this research work. P.B.D. also acknowledges the Council of Scientific and Industrial Research, India for financial support. We sincerely thank Jay Ghatak and Dr. P. V. Satyam of the Institute of Physics, Bhubaneswar, India for help in carrying out the HRTEM measurements.

*Corresponding author. Email address: brmehta@physics.iitd.ernet.in

[1] Al. L. Efros and M. Rosen, Annu. Rev. Mater. Sci. **30**, 475 (2000).
[2] A. A. Lipovskii, E. V. Kolobkova, and V. D. Petrikov, Phys. Solid State **40**, 794 (1998).
[3] A. Tomasulo and M. V. Rama Krishna. Chem. Phys. **210**, 55 (1996).
[4] M. S. Han, T. W. Kang and T. W. Kim, Appl. Surf. Sci. **140**, 1 (1999).
[5] J. T. Benhlal, K. Strauch, K. Granger, and R. Triboulet, Opt. Mater. **12**, 143 (1999).
[6] A. A. Lipovkii *et al.*, J. Non-Cryst. Solids **221**, 18 (1997).
[7] P. Lefebvre, T. Richard, H. Mathieu, and J. Allegre, Solid State Commun. **98**, 303 (1996).
[8] K. Tsunetomo, H. Nasu, H. Kitayama, A. Kawabuchi, Y. Osaka, and K. Tikayama, Jpn. J. Appl. Phys., Part 1 **28**, 1928 (1989).
[9] B. G. Potter and J. H. Simmons, Phys. Rev. B **43**, 2234 (1991).
[10] R. Reisfeld J. Alloys Compd. **341**, 56 (2002).
[11] Y. Masumoto and K. Sonobe, Phys. Rev. B **56**, 9734 (1997).
[12] J. Yang, X.-L. Yang, S. H. Lu, X.-M. Liu, and Y.-T. Qian, Mater. Res. Bull. **35**, 1509 (2000).
[13] Powder Diffraction File, Joint Committee on Powder Diffraction Standards, ASTM, Philadelphia, PA, 1967, Card 150770 (cubic CdTe).
[14] P. Babu Dayal, B. R. Mehta, and S. M. Shivaprasad, Jpn. J. Appl. Phys., Part 1 (to be published October 2005).
[15] Heibelberg in II-VI compounds in *Landolt-Börnstein: Numerical Data and Functional Relationships in Science and Technology*, edited by O. Madelung, Vol. 22, Pt. A (Springer, Berlin 1982), p. 175.
[16] C. M. Herzinger and B. D. Johs, U.S. Patent No. 5796983 (1998).
[17] P. D. Paulson, B. E. Mc Candless, and R. W. Birkmire, J. Appl. Phys. **95**, 3010 (2004).
[18] P. D. Paulson, W. N. Shaferman, and R. W. Birkmire, J. Appl. Phys. **94**, 879 (2003).
[19] P. Babu Dayal, B. R. Mehta, S. M. Shivaparasad, and Y. Aparna, Appl. Phys. Lett. **81**, 4254 (2002).
[20] E. D. Palik, *Optical Constants of Solids* (Academic Press, New York, 1978), Vol. 1.
[21] S. Adachi, T. Kimura, and N. Suzuki, J. Appl. Phys. **74**, 3435 (1993).
[22] U. Woggon, *Optical Properties of Semiconductor Quantum Dots* (Springer, Berlin, 1997).
[23] R. Tsu and D. Babic, Appl. Phys. Lett. **64**, 1806 (1994).
[24] V. Ranajan and V. A. Singh, J. Appl. Phys. **89**, 6415 (2001).
[25] K. Wei, F. H. Pollak, J. L. Freeouf, D. Shvydka, and A. D. Compaan, J. Appl. Phys. **85**, 7418 (1999).
[26] P. Lautenschlager, S. Logothetidis, L. Vina, and M. Cardona, Phys. Rev. B **32**, 3811 (1985).
[27] Rossler in II-VI compounds in *Landolt-Börnstein: Numerical Data and Functional Relationships in Science and Technology*, edited by O. Madelung, Vol. 22, Pt. A (Springer, Berlin 1982), p. 211.
[28] J. Perez Conde *et al.*, Phys. Rev. B **64**, 113303 (2001).
[29] J. H Simmons, J. Non-Cryst. Solids **239**, 1 (1996).
[30] M. J. Yacaman, J. S. Ascencio, H. B. Liu, and J. Gordea-Torresday, J. Vac. Sci. Technol. B **19**, 1091 (2001).
[31] S. H. Tolbert and A. P. Alivisatos, Annu. Rev. Phys. Chem. **46**, 595 (1995).
[32] K. K. Nanda, S. N. Sahu, and S. N. Behra, Phys. Rev. A **66**, 013208 (2002).
[33] C. Q. Sun *et al.*, J. Phys.: Condens. Matter **14**, 7781 (2002).
[34] D. G. Thomas, J. Appl. Phys. **32**, 2298 (1961).
[35] L. N. Alejo-Armenta *et al.*, J. Phys. Chem. Solids **60**, 807 (1999).
[36] J. J. Hopfield J. Appl. Phys. **15**, 97 (1960).
[37] Kenneth Zanio, *Cadmium Telluride*, Semiconductors and Semimetals Vol. 13 (Academic Press, New York, 1978).
[38] M. Allais and M. Gandais, Philos. Mag. Lett. **65**, 243 (1992).
[39] T. V. Buuren, L. N. Dinh, L. L. Chase, W. J. Siekhaus, and L. J. Terminello, Phys. Rev. Lett. **80**, 3803 (1998).
[40] B. Balamurugan, I. Aruna, B. R. Mehta, and S. M. Shivaprasad, Phys. Rev. B **69**, 165419 (2004).